Supplementary Data:

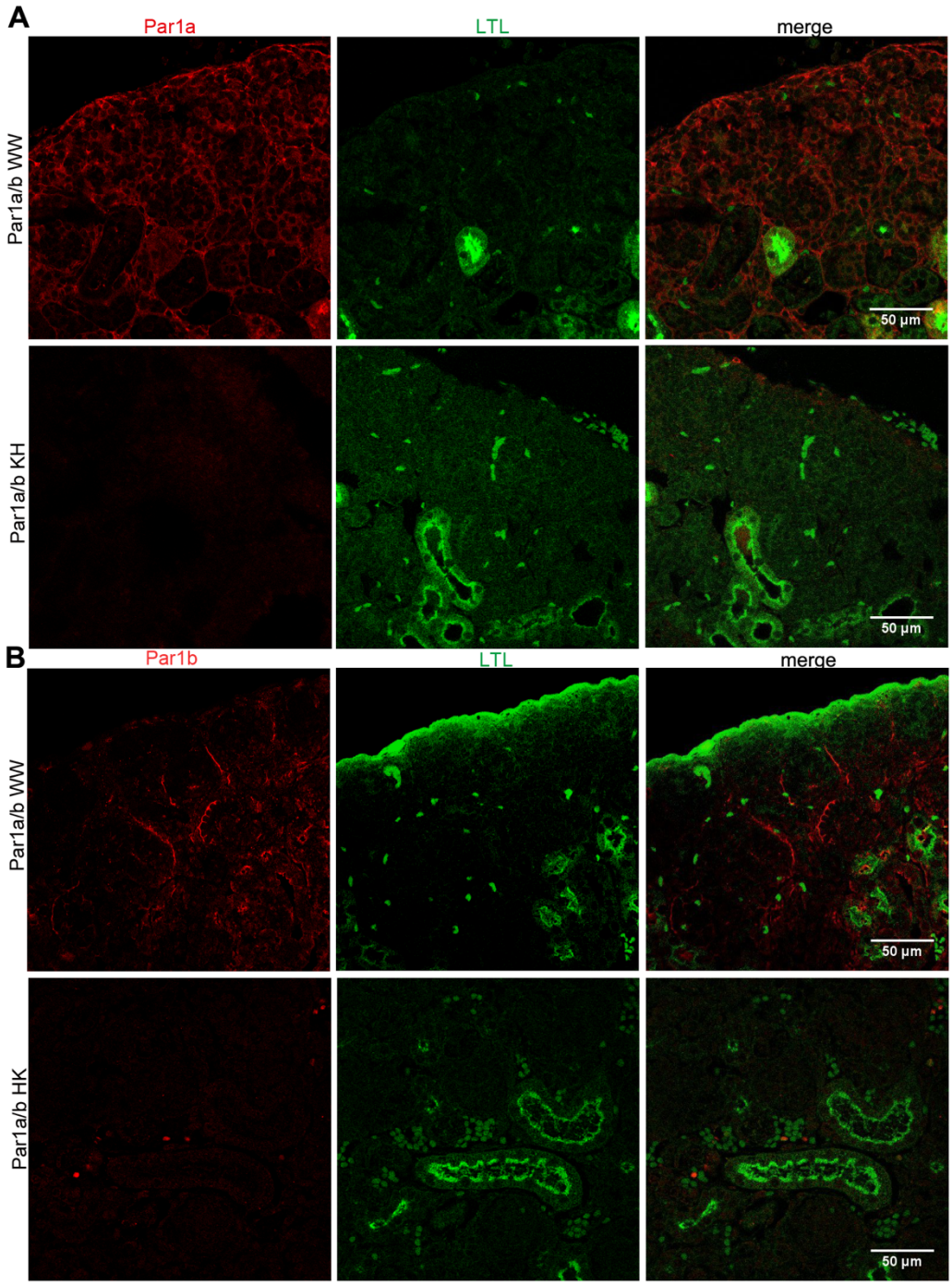

Fig. S1: Homologue specific antibodies for Par1a and Par1b

IHC for Par1a **(A)** and Par1b **(B)** co-stained with LTL in newborn wild type and mutant mouse kidneys: **A)** Par1a is expressed in the periphery (nephrogenic cortex) of Par1a/b WW mouse kidneys. No Par1a expression is identified in Par1a/b KH kidneys, demonstrating specificity of the Par1a antibody. **B)** Par1b is expressed in the periphery (nephrogenic cortex), and unique membrane Par1b expression is present in developing glomeruli. No Par1b is expressed in Par1a/b HK kidneys, demonstrating specificity of the Par1b antibody.

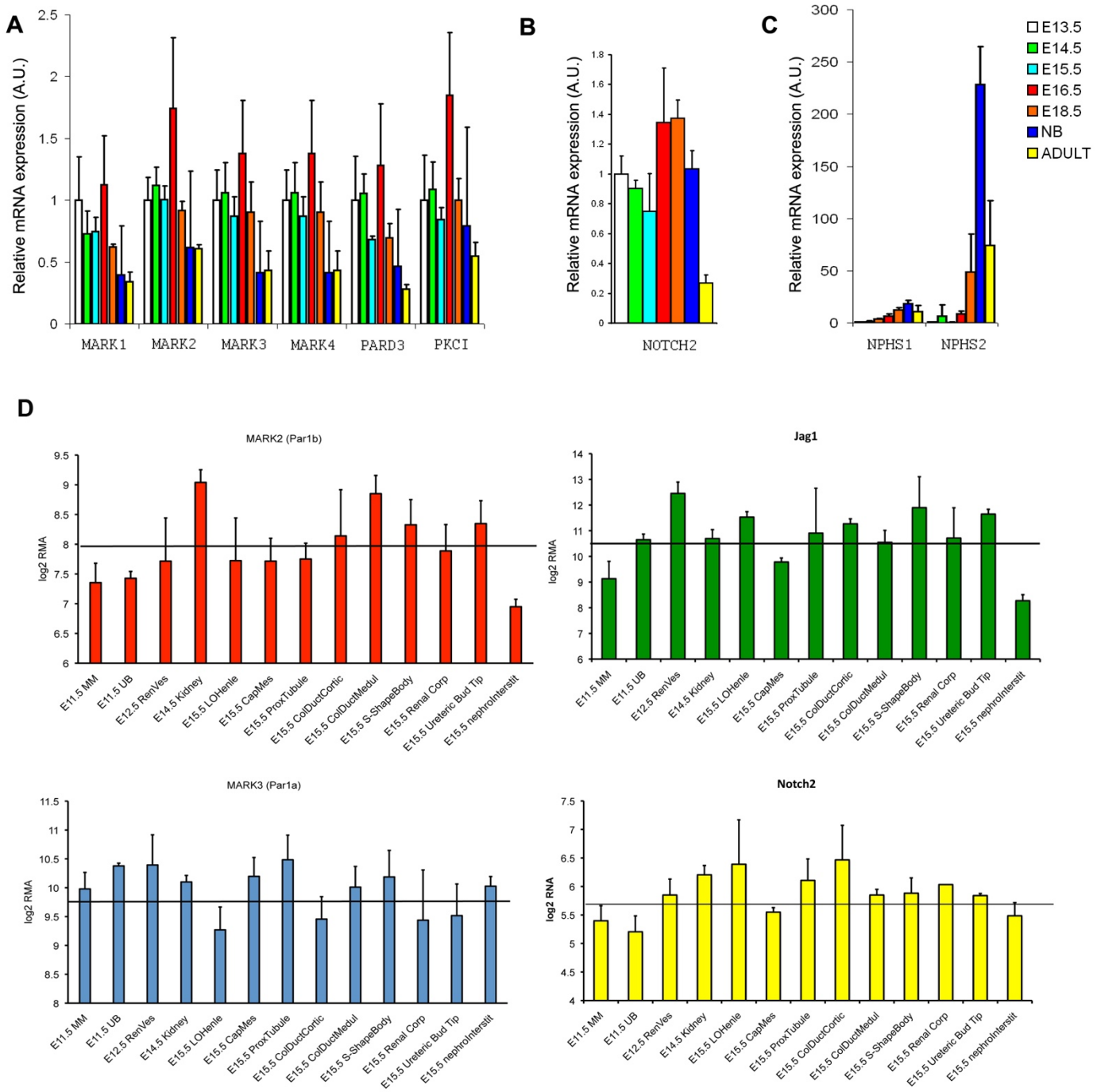

Fig. S2:

Embryonic expression of Par1a/b proteins coincides with Notch pathway, and precedes *Nphs1* and *Nphs2* expression.

A-C) Real-time PCR demonstrating differences in the mRNA expression during development in embryonic (E), newborn (NB1), and adult rat kidneys. **A)** mRNA for *Par1a (MARK3*) and *Par1b* (*MARK2*) (*MARK1-4*), *Pard3* (*PARD3*), and atypical protein kinase C (*aPKC/ PRKCI*) expression is higher in developing as compared to adult kidneys **B)** *Notch2* expression pattern is similar to *Par1/Pard3/aPKC* expression **C)** Terminal

differentiation markers, such as *Nphs1* and *Nphs2*, are highly expressed later during development and in the adult kidney. Data represent the S.E.M. per time-point. mRNA for embryonic time-points was isolated from pooled embryonic kidneys. D) Microarray data from the GUDMAP database demonstrating mRNA expression profiles (log2RNA, mean ± standard deviation) of *MARK2* (*Par1b*), *MARK3* (*Par1a*), *Jag1* and *Notch2* in microdissected embryonic mouse kidneys. Line indicates median expression, such that bars above line indicate increased expression above median (red on microarray data). Note that rat embryonic kidney development lags approximately 1 day behind mouse. Peak expression of *MARK2* (*Par1b*) is in the S-shape body, collecting duct and ureteric bud tip. Peak expression of *MARK3* (*Par1a*) is in the S-shape body, proximal tubules, and early ureteric bud (E11.5). Peak *Jag1* expression is also in the S-shape body, ureteric bud tip, proximal tubule and collecting duct. Peak *Notch2* expression is in the renal vesicle, loop of Henle, S-shape body, ureteric bud tip and collecting ducts.

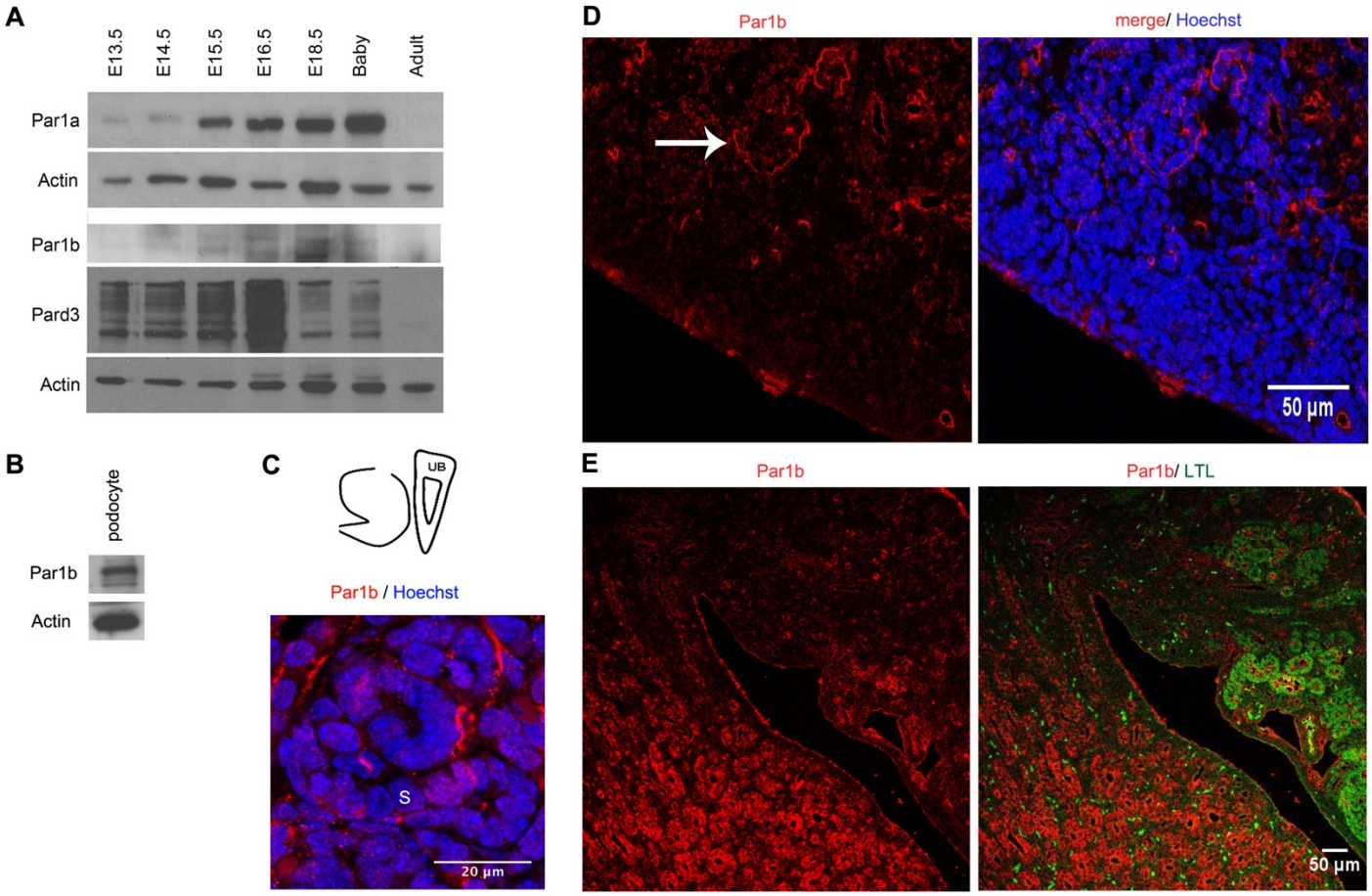

Fig. S3

Par1a/b expression is increased in developing nephrons. A) Western blot demonstrating that protein expression correlates with Par1a and Par1b mRNA expression (as depicted in Fig. S2), with peak expression of Par1 proteins in the developing rat kidney at approximately embryonic day 18.5. Pard3 expression appears increased earlier in development. Adult rat kidneys have decreased expression of Par1a and 1b as compared to embryonic kidneys. Par1b has 2 bands and Pard3, 3 bands, that are due to multiple splice isoforms. **B)** Western blot for Par1b on cultured immortalized podocytes lysates, demonstrating strong podocyte expression of Par1b **C,D,E)** IHC for Par1b in mouse kidneys**: C)** Par1b is expressed in mouse S-shape (S) body**. D)** IHC for Par1b demonstrating expression in developing mouse glomeruli (D, arrow) and renal papilla (E).

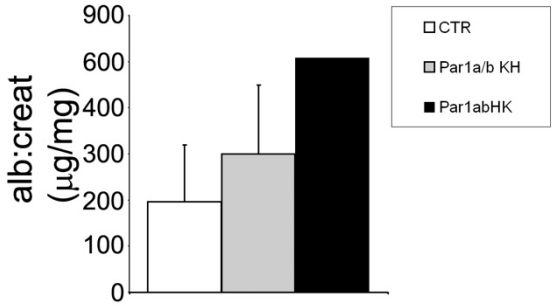

Fig. S4

Albumin:creatinine ratios in Par1a/b mutant and control mice

Albumin:creatinine ratio is higher in Par1a/b HK mutant urine (n=1, rest of 8 total mutants had insufficient urine) versus Par1a/b KH urine (n=3, rest of 16 total mutants with insufficient urine) and controls (18/22 with urine). Small sample size precludes statistical analysis.

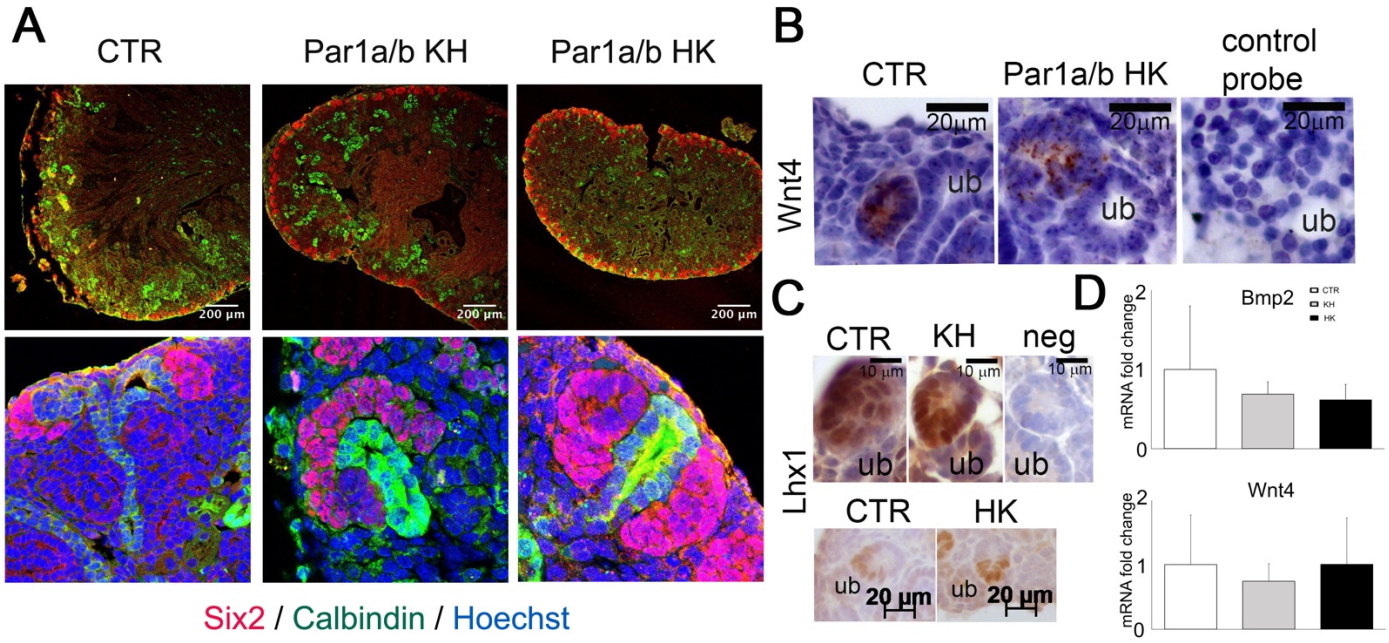

Fig. S5 Nephron progenitors and early differentiation into renal vesicles are preserved in Par1a/b mutant kidneys

A) Immunostaining for Six2 (red) and calbindin (green) demonstrating maintenance of nephron progenitors in Par1a/b mutants. Lower panels are higher magnification. **B)** In situ hybridization for *Wnt4* demonstrating similar expression in Par1a/b HK mutants vs. controls. **C)** Immunostaining for Wnt target Lhx1 demonstrating similar patterns of Lhx1 expression in cells of renal vesicles adjacent to the ureteric bud in Par1a/b KH and HK mutants vs. controls **D)** Real time PCR demonstrating no change in overall *Wnt4* or *Bmp2* expression in Par1a/b mutants vs. control (CTR) newborn kidneys (p=NS).

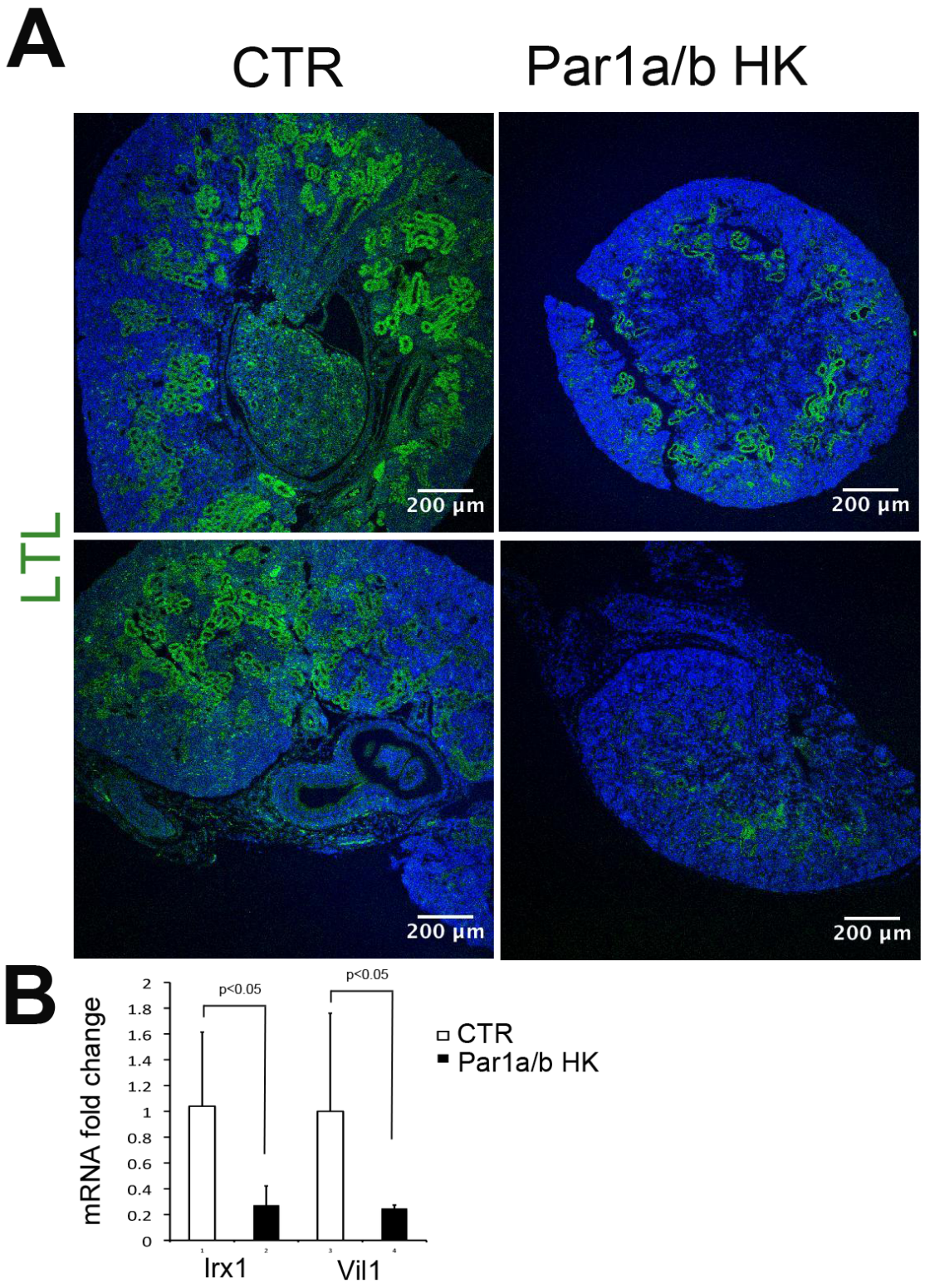

Fig. S6:

Proximal tubular formation is impaired in Par1a/b HK kidneys

A) LTL labeling of proximal tubules (green) demonstrating decreased LTL positive tubules in Par1a/b HK vs. controls (CTR). B) Real time PCR for proximal tubular genes (*Irx1* (expressed in the S3 segment) and *Vil1*) demonstrating decreased proximal tubular gene expression in Par1a/b HK kidneys vs. controls.

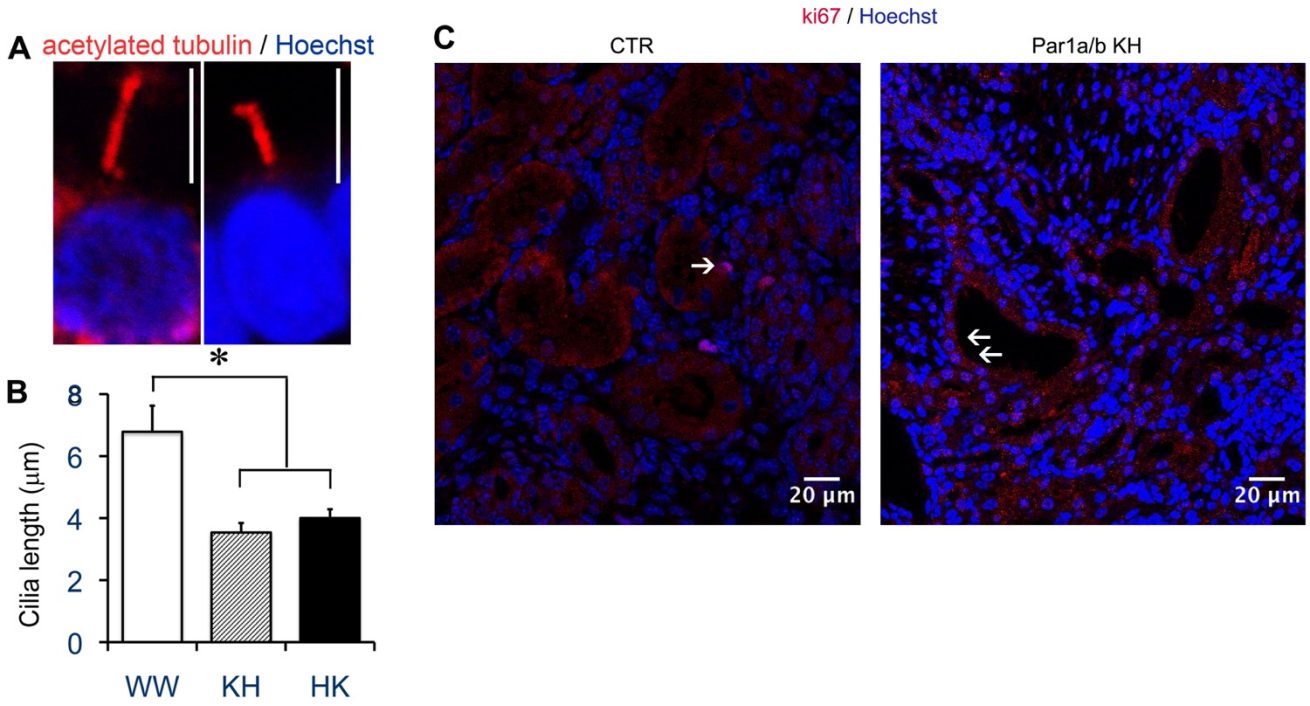

Fig. S7 Par1a/b mutants exhibit shorter cilia and proliferation in cystic tubules

A) Immunostaining for acetylated tubulin identifies cilia. Par1a/b mutants exhibit shortened cilia. **E** Quantification confirms decreased cilia length in mutants vs. wild-type (WW), *p<0.04.

B) Immunostaining for Ki-67 (red) merged with Hoechst (blue) demonstrates tubular proliferation (pink, arrows). Cystic tubules have evidence of proliferation (arrows). Occasional proliferating nuclei are observed in control newborn tubules.

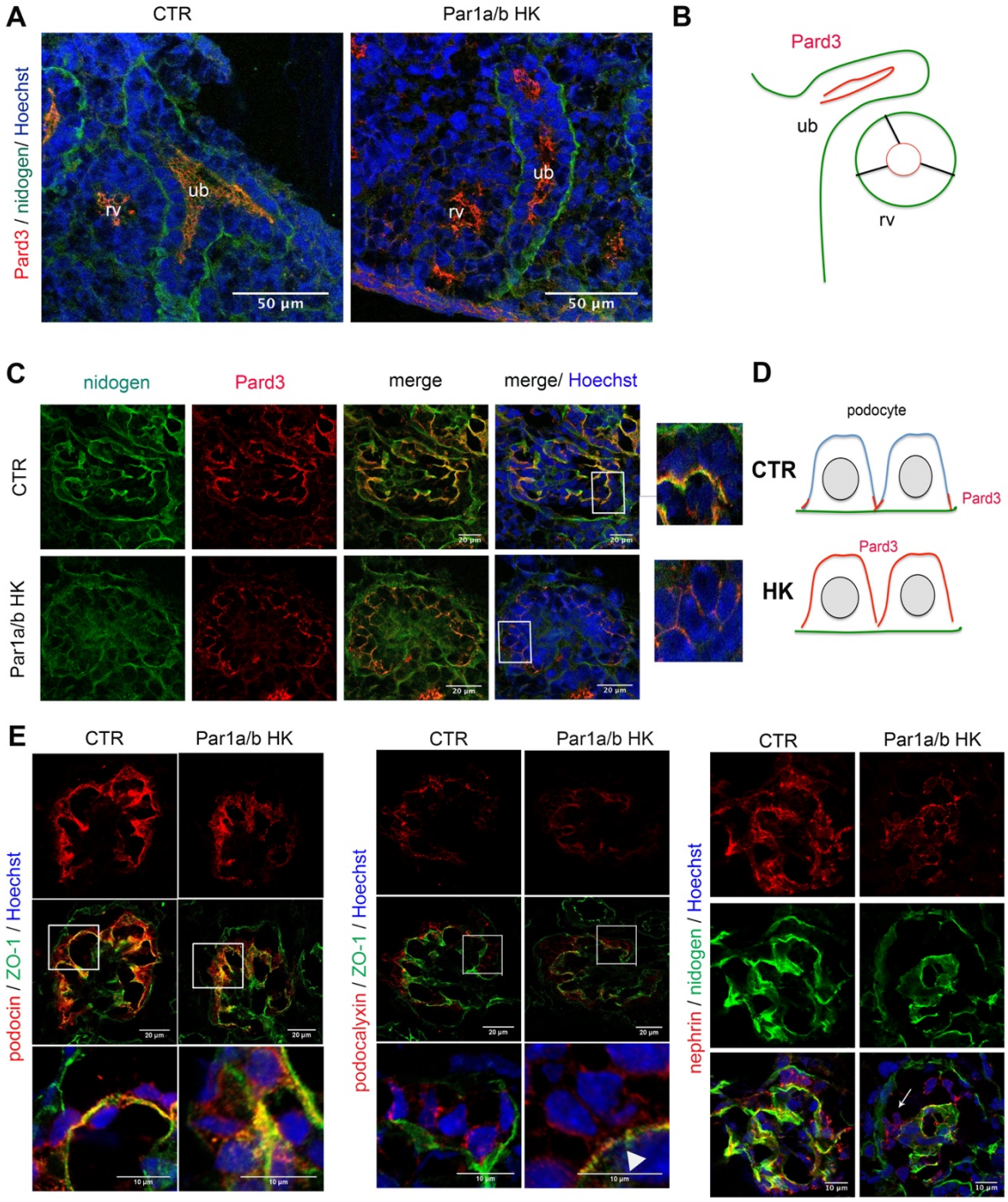

Fig. S8: Pard3 localization is intact in early differentiating Par1a/b HK renal epithelial structures, but not developing glomeruli

Immunostaining for Pard3 (red) and basement membrane nidogen (green) was performed in E15.5 kidneys and control (CTR) littermates **(A, C)**. **A)** Pard3 localizes to apical membranes in developing renal vesicle (rv) and ureteric bud (ub) (depicted in schema **B)** in both Par1a/b HK kidneys and littermate controls. **C)** In mature control glomeruli, Pard3 has migrated down to co-localize with the nidogen positive glomerular basement membrane (yellow in merge). In Par1a/b HK glomeruli, Pard3 retains an immature expression pattern and remains on the apical membrane of developing podocytes. White box insets shown enlarged to right. **D** depicts

schema of normal and altered Pard3 expression. E) Immunostaining for podocin and ZO-1 (left), podocalyxin and ZO-1 (middle) and nephrin and nidogen (right). In controls, podocin and nephrin strongly colocalizes at the glomerular basement membrane with ZO-1 and nidogen, respectively (yellow in merge images, white boxes indicate areas enlarged below), whereas podocalyxin is fully localized to the apical podocyte membrane and fully segregates from the ZO-1 staining. In Par1a/b HK glomeruli, less co-localization of podocin and nephrin with ZO-1 and nidogen is observed. In addition, podocalyxin expression co-localizes with ZO-1 (arrowhead in enlarged inset). Arrow points to abnormal disorganized heap of podocytes with diffuse membrane expression of nephrin in Par1a/b HK glomeruli.

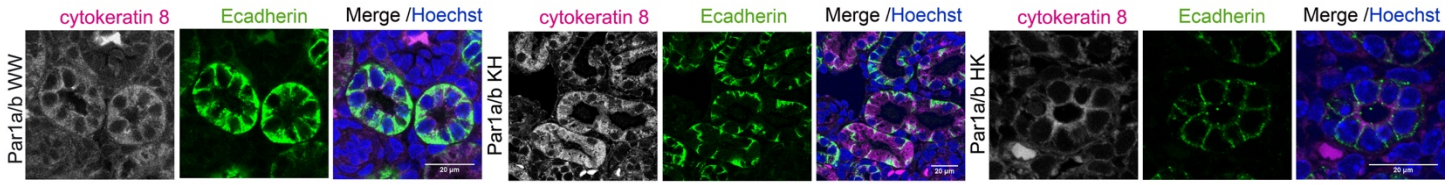

Fig. S9

Polarized expression of E-cadherin is preserved in Par1a/b distal tubules.

Cytokeratin 8 and E-cadherin localize to the basolateral aspect of distal tubules in Par1a/b WW, KH, and HK kidneys (IHC).

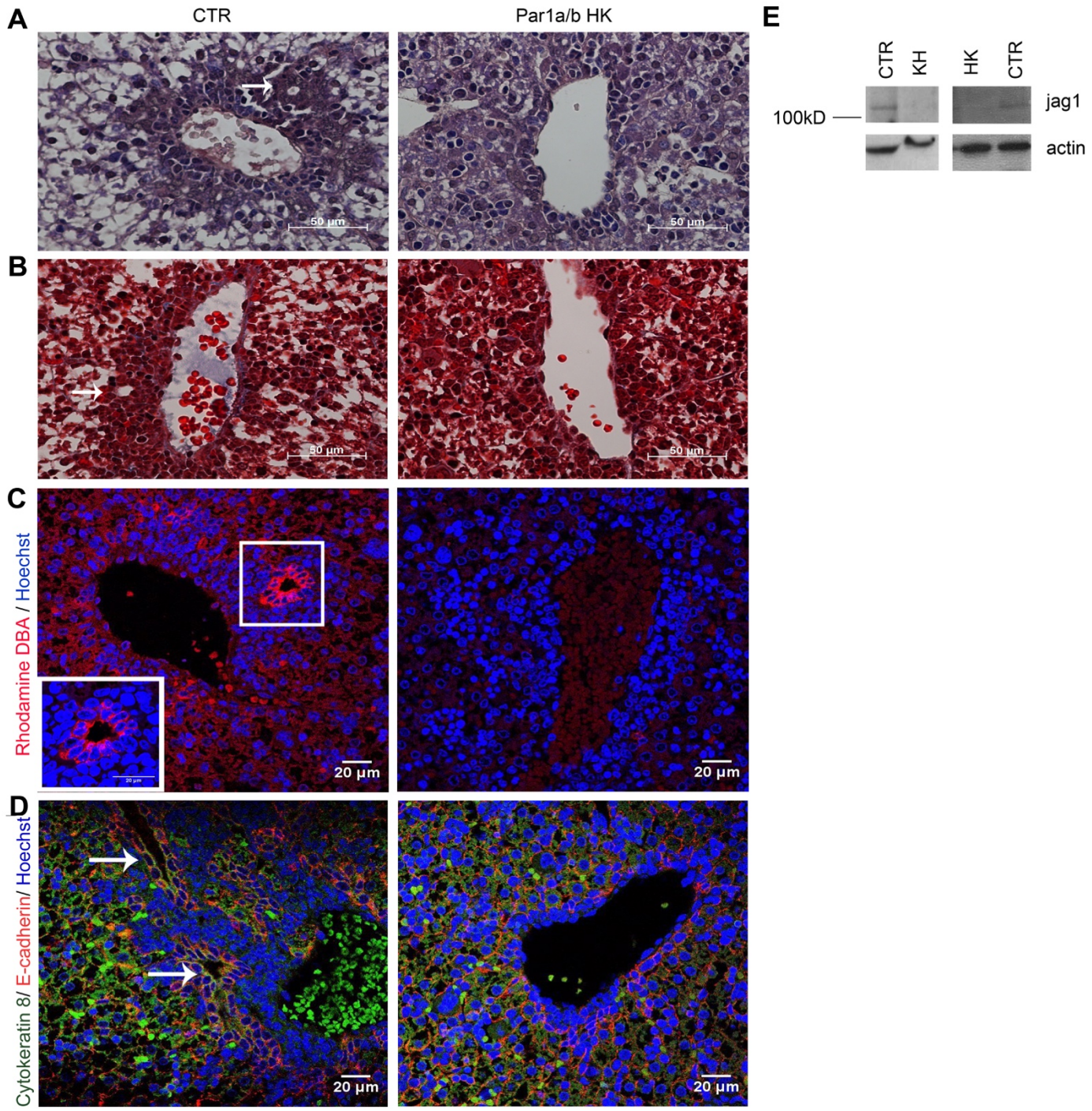

Fig. S10 Paucity of bile ducts in Par1a/b HK livers associated with decreased Jag1 expression

PAS (**A**) and Trichrome (**B**) staining demonstrating bile ducts (arrows) around portal veins in the control newborn livers (left panel) and lack of bile ducts surrounding portal veins in Par1a/b HK newborn livers (right panel). Immunostaining for bile duct markers Rhodamine DBA (**C**) and Cytokeratin 8 (**D**) confirms lack of bile ducts (arrows) in Par1a/b HK livers. In controls, approximately 1.3 ± 0.16 bile ducts identified per portal vein

cross-section. In contrast, well-formed bile ducts were completely absent in surrounding portal veins Par1a/b HK livers. Par1a/b KH livers had a more variable, intermediate phenotype, with 0.6 ± 0.6 bile ducts identified per portal vein cross section (p=NS vs. Par1a/b WW). **E)** Western blots for Jag1 demonstrating decreased expression in Par1a/b KH and HK E18 livers as compared to littermate controls.

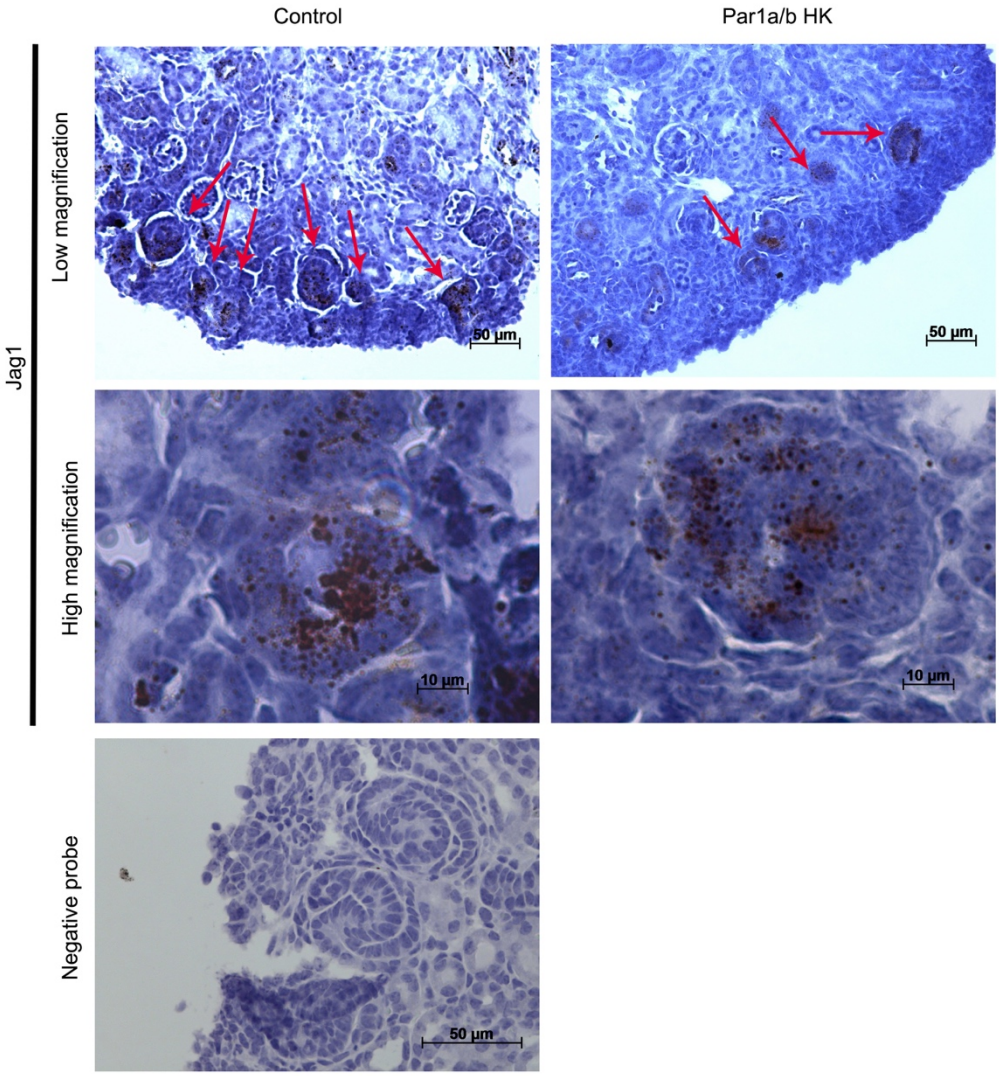

Fig. S11 Less Jag1 mRNA is detected in Par1a/b embryonic mutant S-shape bodies

Jag1 ISH demonstrating overall weaker staining and decreased number of Jag1 positive S-shape bodies in Par1a/b E18.5 mutants (arrows indicate Jag1 staining in low magnification view). Jag1 mRNA is not completely lost Par1a/b mutant S-shape bodies (middle panels), but larger brown staining in controls indicates greater expression. Bottom panel demonstrates negative control probe.

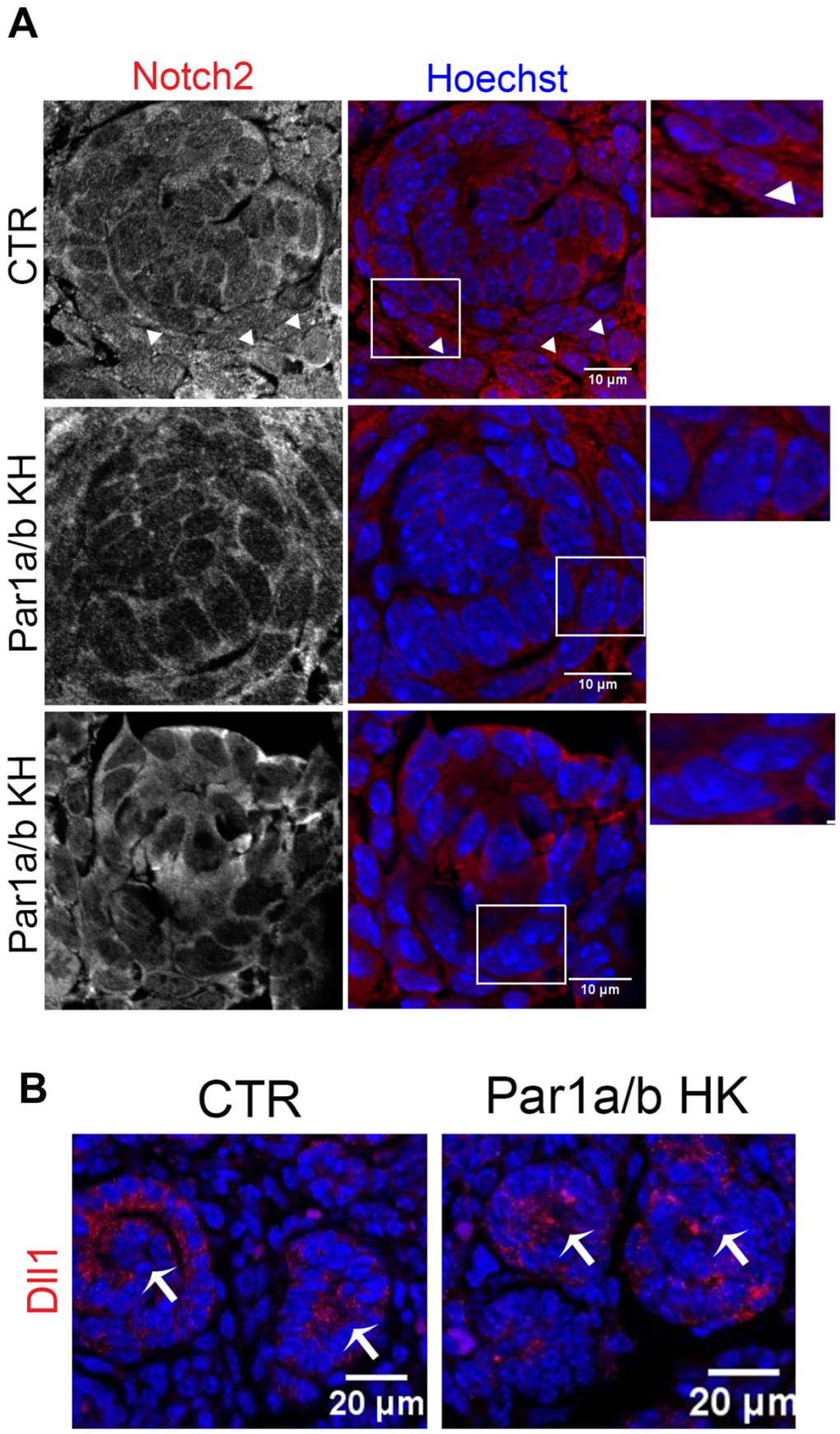

Fig. S12 Notch2 localization in Par1a/b mutant S-shape bodies indicate less activated, nuclear Notch2

Immunostaining for Notch2 **(A)** and Dll1 **(B)** was performed in newborn and embryonic E18.5 kidneys. Representative images are shown, enlarged insets to right. Arrowheads indicate nuclear Notch2 (co-localize with Hoechst, pink in enlarged insets to right) in the proximal portion of the S-shape body in controls that is not seen in Par1a/b mutants (KH and HK). **B)** As expected, Dll1 is less strongly expressed than Notch2 or Jag1 and localizes to mid-portion of the S-shape body (white arrows), as previously described[1]. Dll1 expression in Par1a/b HK mutant S-shape bodies appears slightly decreased compared to controls.

Supplementary Table Oligonucleotide sequences for real time PCR

Primer name	Primer sequence (5'-3')	
	Forward	Reverse
m-Jag1	AGC GGA CTT TCT GCT GGT GT	ACT CGG AAG TGG AGG AGG ATG
m-FoxD1	CCC CTC CTG GAC TAA CCG GGC	CGA GGT GTT TTG CGC TCC CCG
m-Ubiquitin	GCC CAG TGT TAC CAC CAA GAA G	GCT CTT TTT AGA TAC TGT GGT GAG GAA
r-MARK1	ATG TCG GCG CGG ACG CCA TT	GGT TCT CCG TGT CCC GCT CG
r-MARK2	CCA TGC TGG GCA GCT CCG AC	TGG GGT CAC ACC GAA GGG CA
r-MARK3	TAG GAC CCC TTT GCC AAC GGT GA	TCT ACA CCG AGC TCC AGA GCG C
r-MARK4	ATG TCT TCG GAG GAC GGC GCT	GCC CAA GGT GCC ATG CGT GT
r-PARD3	CCA CCG AGG GCA ACA AGC GT	CCA CCG AGG GCA ACA AGC GT
r-PKCI	TGC CCA GGG GAA GAC AAG TCC A	AGA TGG CAC AGT GGG CAC GC
r-Notch2	CTG TTG TCA GTG AAT CGG AGG AT	CAG CAA CCG CAA GCA GAT AG
r-NPHS1	GTG GAC TGG GGA CCG GGA CA	TTG GGG GAA GCT GGG GGC TG
r-NPHS2	GCC AGC TGG GCT TCA GCA CT	TTC GGC AGC AAT CAC CCG CA
r-Ubiquitin	TGC AGC CAA CAC CGC TGA CAA	GGG GGA TGC CCT CCT TGT CCT

Supplementary methods:

Antibodies used for Western blot: We used the following primary antibodies: mouse anti-C-TAK1 (Par1a, Upstate 05-680), goat anti-MARK2 (Par1b, Abcam 77641), rabbit anti-Par3 (Millipore 07-330), goat anti-Jagged1 (C-20, Santa Cruz, 6011 and Abcam ab109635), rabbit anti-actin (Sigma-Aldrich A 2066), rabbit anti-Notch2, cleaved N terminus (N2ICD, Millipore 07-1234), rabbit anti-Hes1 (Millipore AB 5702).

Antibodies used for immunohistochemistry:

We used the following primary antibodies: mouse anti-acetylated tubulin (Sigma-Aldrich, T7451), rat anti-cytokeratin 8 (Troma I, Developmental hybridomas), mouse anti-beta-catenin (BD Transduction Laboratories), goat anti-E-cadherin (R&D systems, AF748), goat anti-Jagged1 (C-20, Santa Cruz, 6011), rabbit anti-Lrp2 (megalin, Abcam 76969), mouse anti Lhx1 (Developmental Hybridoma, 4F2), rabbit anti Dll1 (Abcam 84620), rabbit anti Notch2 (Abcam 8926), rabbit anti-Pax-2 (Invitrogen, 71-6000), rabbit anti-SIX2 (Proteintech, 11562-1-AP), goat anti-podocalyxin (R&D, AF1556), rat anti-Nidogen (Millipore, ELM1), mouse anti-C-TAK1/MARK3 (Par1a, LS Bio 5226), rabbit anti-MARK2 (Par1b, Novus Biologicals P1-64759), guinea pig anti Nephrin (Fitzgerald, 20R-NP002), and rabbit anti podocin (Sigma, P0372). For lectin stains, FITC-lotus tetragonolobus

lectin (LTL) or Flourescein or Rhodomine dolichos DBA (Vector labs: 1:50) were applied. Nuclei were stained with Hoechst (Sigma).

Real time PCR: Rat embryonic kidney RNA was isolated from pooled embryonic kidneys (15-25 kidneys/pool) of littermates using Qiagen (Valencia, CA) RNeasy Mini Kit with DNase I digestion performed on-column using the RNase-Free DNase Set as per manufacturer's instructions. Newborn mouse kidney RNA was isolated from individual kidneys (3-5 per genotype), using TRIzol reagent (Invitrogen) per manufacturer's instructions. Real time PCR was performed with the following program: 50 °C for 2 min, 95 °C for 10 min, 40 cycles of 95 °C for 10 sec, 55 °C for 20 sec, 72 °C for 30 sec, followed by 95 °C for 15 sec, 60 °C for 15 sec, and 95 °C for 15 sec. Primers were designed using NCBI Primer-BLAST (Supplementary Table 1) or published primers.[2-4] Relative mRNA expression was determined using the $\Delta\Delta$ Ct method [5] with expression of ubiquitin (UBC) as the housekeeping control. Each time point was assayed by examining 3 sets of pooled embryonic rat kidneys and 3-5 newborn Par1a/b pups, and experiments were performed in duplicate. Results were expressed normalized to the average of three sets of pooled E13.5 rat kidneys or to average of 3-5 Par1a/b WW newborn mouse kidneys. GUDMAP microarray data was obtained from GUDMAP database: http://www.gudmap.org.

Transmission electron microscopy: Mid-sagittal sections were obtained and the deepest, most mature glomeruli were examined. Sample was fixed with 2.0% paraformaldehyde and 2.5% glutaraldehyde in 0.1 M sodium cacodylate buffer, postfixed with 1% osmium tetroxide followed by 1% uranyl acetate, dehydrated through a graded series of ethanol and embedded in Spurrs resin (Electron Microscopy Sciences, Hatfield, PA). Ultrathin sections were cut on a Reichert Ultracut UCT, stained with uranyl acetate followed by lead citrate and viewed on a JEOL 1200EX transmission electron microscope at 80kv.

Albumin and creatinine ratio:

Urine was obtained by bladder puncture. Urine albumin and creatinine was measure by Albuwell M Elisa and Exocell creatinine assays, respectively as per manufacturers instructions.

In situ hybridization: In situ hybridization (ISH) was performed using ACD Biosystems Brown kit and commercially available mouse Hes1, Jag1, Wnt4 and control probes as per manufacturers instructions.

Cilia length measurement:

Newborn mouse kidneys were immunostained for acetylated tubulin as described above and sections reviewed under the confocal microscope with high magnification. Acetylated tubulin immunostained cilia were visualized with the confocal microscope. Examination was made to determine that the cilia did not leave the plane of the confocal image. Only cilia with their length entirely within the plane were imaged and length was measured with Image J software (NIH). At least five sections were analyzed per genotype.

Glomerular number quantification:

Mid-sagittal sections were obtained from formalin-fixed paraffin-embedded newborn mouse kidneys and stained with H&E. Mature glomeruli were then counted in at least three different pups per genotype.

Ureteric bud branching: E12.5 kidneys were dissected out and fixed in 4% PFA for one hour. After PBS-Tween 0.1% washes, kidneys were blocked in PBS with 2%BSA, 0.1%Tween. Primary antibody cytokeratin 8 (Troma I antibody, Developmental hybridomas) was applied and left overnight. After washing appropriate secondary antibodies were applied and images were obtained. Primary (main) branches were counted with a minimum of 3 kidneys per genotype. Littermates were used as controls.

Tubular dilation classification:

Brightfield images of Par1a/b controls and mutant kidneys were analyzed using Image J as per protocol described by Bastos et al.[6] Briefly, a grid of dots 13 μm apart was superimposed on images. Tubular dilation was scores as no dilation (no dots within lumen), tubular dilation I (TD I, one dot within tubular lumen), tubular dilation II (TD II, two dots within lumen), microcyst (3-9 dots within lumen), and cyst (10 or more dots within lumen). Data was expressed as percentage of total tubular lumens quantified.

Bile duct quantification:

Sections stained for Rhodamine DBA and cytokeratin 8 were viewed under fluorescent microcopy. All portal veins per section were examined for the presence of labeled bile ducts (n>3 mice/ group, with >10 portal veins cross-sections visualized/ mouse).

Additional References:

1. Liu, Z, Chen, S, Boyle, S, Zhu, Y, Zhang, A, Piwnica-Worms, DR, Ilagan, MX, Kopan, R: The extracellular domain of Notch2 increases its cell-surface abundance and ligand responsiveness during kidney development. *Developmental cell,* 25**:** 585-598, 2013.
2. Niranjan, T, Bielesz, B, Gruenwald, A, Ponda, MP, Kopp, JB, Thomas, DB, Susztak, K: The Notch pathway in podocytes plays a role in the development of glomerular disease. *Nature medicine,* 14**:** 290-298, 2008.
3. Heliot, C, Desgrange, A, Buisson, I, Prunskaite-Hyyrylainen, R, Shan, J, Vainio, S, Umbhauer, M, Cereghini, S: HNF1B controls proximal-intermediate nephron segment identity in vertebrates by regulating Notch signalling components and Irx1/2. *Development (Cambridge, England),* 140**:** 873-885, 2013.
4. Murea, M, Park, JK, Sharma, S, Kato, H, Gruenwald, A, Niranjan, T, Si, H, Thomas, DB, Pullman, JM, Melamed, ML, Susztak, K: Expression of Notch pathway proteins correlates with albuminuria, glomerulosclerosis, and renal function. *Kidney international,* 78**:** 514-522, 2010.
5. Livak, KJ, Schmittgen, TD: Analysis of relative gene expression data using real-time quantitative PCR and the 2(-Delta Delta C(T)) Method. *Methods (San Diego, Calif),* 25**:** 402-408, 2001.
6. Bastos, AP, Piontek, K, Silva, AM, Martini, D, Menezes, LF, Fonseca, JM, Fonseca, II, Germino, GG, Onuchic, LF: Pkd1 haploinsufficiency increases renal damage and induces microcyst formation following ischemia/reperfusion. *Journal of the American Society of Nephrology : JASN,* 20**:** 2389-2402, 2009.